# BEHAVIOUR OF PULTRUDED GFRP CHANNEL BEAMS UNDER TRANSVERSE LOADING

**[1]JYOTIRMOY HALOI, [2]ARUN CHANDRA BORSAIKIA, [3]KONJENGBAM DARUNKUMAR SINGH, [4]SUMAN KUMAR MUSHAHARY**

[1]Department of Civil Engineering, National Institute of Technology Silchar, India
[2,3,4] Department of Civil Engineering, Indian Institute of Technology Guwahati, India
E-mail: [1]jyotirmoy@civil.nits.ac.in, [2]arubors@iitg.ac.in, [3]darun@iitg.ac.in, [4]tsumn@iitg.ac.in

**Abstract** - Glass Fibre Reinforced Polymer (GFRP) beams often encounter web crippling failure under transverse loading. In case of unsymmetrical sections such as channel beams, however, limited studies are reported. In the present investigation, behaviour of GFRP channel profiles under transverse bearing load has been assessed considering end-two-flange (ETF) and interior-two-flange (ITF) loadings. Experimental program comprised mechanical characterization tests and web crippling experiments conducted on 12 specimens extracted from three channel profiles. Primarily, effect of web slenderness ratio and effect of varying loading conditions on the web crippling behaviour were investigated. Two failure modes, namely, web crushing and web buckling failure were observed in the specimens. In addition, it was found that changing loading condition from ETF to ITF increased the ultimate crippling capacity of the specimens by upto +184.7%.

**Keywords** - Pultruded GFRP Channel Profile; Web Crippling; Web Buckling; Bearing Length.

## I. INTRODUCTION

Pultruded glass fibre reinforced polymer (GFRP) composite sections are increasingly used as structural members instead of steel and concrete members owing to advantages such as corrosion resistance, high strength to weight ratio, availability in different shapes and sizes, low cost of production etc. Highway bridges, pedestrian bridges, gable frame buildings, cooling towers etc. have been built utilizing these composite members [1–3]. Having said that, it can be noted that instability caused by buckling and less fire resistance are some of the main limitations restricting their extensive use [1–5]. Pultruded profiles are produced by the method called pultrusion, where, the fibre rovings are pulled in pultrusion or longitudinal direction leaving the tranverse direction of the profiles with lower mechanical properties. Due to this reason, web crippling failure is often observed in GFRP beams under transverse loading and is mainly characterised by crushing of web, web-flange junction separation and web buckling [3–8].

Study on the web crippling phenomena of GFRP sections is limited compared to steel sections. Influence of a range of parameters on web crippling behaviour has been investigated. These primarily include slenderness ratio [4, 6–8], bearing length [3–12], loading and support boundary conditions [3–4], perforation in web [6–7] etc. Researchers have considered various cross-sectional shapes such as rectangular hollow section, I-shaped sections, channel beams etc. and design rules are proposed by utilizing the data obtained in those studies. In case of channel beams, however, very limited studies are reported [4, 12]. Henceforth, additional studies are needed to gain better insight into the failure mechanism and to establish more general design rule with greater reliability.

In this paper, an attempt has been made to investigate the performance of GFRP channel profiles under transverse bearing load. Mainly, effect of web slenderness ratio and effect of loading conditions on the behaviour of channel beams have been studied. Experimental investigation comprised mechanical characterization tests along with full scale web crippling testing of GFRP channel sections considering two flange loading configurations: end-two-flange (ETF) and interior-two-flange (ITF). The outcomes of the present investigation are reported in terms of failure modes of the specimens, their load–displacement plots and ultimate loads.

## II. EXPERIMENTAL INVESTIGATION

### 2.1 General

The GFRP channel profiles utilized in the current investigation were procured from an Indian manufacturer. The investigation includes material characterization tests and web crippling experiments. Following sections will discuss the particulars regarding the mechanical characterization tests and web crippling tests.

### 2.2 Material properties

From burn-off test (ASTM D2584 [13]), it was observed that an average glass content of ~72.76% was used to manufacture the GFRP profiles. Various fibre architectures utilized in manufacturing the channel sections are reported in a prior study by the authors [14]. Mechanical characterization of the GFRP profiles were carried out by performing tensile (ASTM D3039 [15]), interlaminar shear (ASTM D2344 [16]), $10^o$ off-axis tension (Hodgkinson, 2000 [17]) and compression (ASTM D3410 [18]) tests. Details of the coupon test results can be found in [14].

| Channel section ID | Width, W (mm) | Height, d (mm) | Flange thickness, $t_f$ (mm) | Web thickness, $t_w$ (mm) | Web slenderness ratio, $\lambda_w$ | Glass fibre content (wt %) |
|---|---|---|---|---|---|---|
| C1 | 29 | 69 | 5 | 5 | 11.8 | 73.78 |
| C2 | 29 | 48 | 3 | 3 | 14.0 | 72.98 |
| C3 | 29 | 79 | 3 | 3 | 24.3 | 71.53 |

**Table 1: Details of GFRP channel section profiles used for the present investigation.**

### 2.3 Web crippling specimens

Web crippling experiments were performed on specimens prepared from three channel profiles of varying web slenderness ratios (see Table 1). Two flange loadings were employed comprising end-two-flange and interior-two-flange loadings. Lengths of the specimens (L) were determined as per the recommendation mentioned in North American Specification (NAS) [19]. The mild steel bearing plates used for transferring the load were of 10 mm thickness with a length (N) of 50 mm. Number of repetition for each set of experiment were kept at two. A total of 12 specimens were tested under two flange loadings and details have been furnished in Tables 2 and 3.

| Specimen ID | Specimen length, L (mm) | Failure modes | Ultimate Load, $P_{EXP}$ (kN) | Average $P_{EXP}$ (kN) |
|---|---|---|---|---|
| C1-ETF-N50-1 | 155 | Web crushing | 9.91 | 10.65 ± 0.74 |
| C1-ETF-N50-2 | 155 | Web crushing | 11.39 | |
| C2-ETF-N50-1 | 125 | Web buckling | 2.77 | 2.83 ± 0.06 |
| C2-ETF-N50-2 | 125 | Web buckling | 2.89 | |
| C3-ETF-N50-1 | 170 | Web buckling | 2.60 | 2.61 ± 0.005 |
| C3-ETF-N50-2 | 170 | Web buckling | 2.61 | |

**Table 2: Failure modes and ultimate web crippling loads in ETF specimens.**

| Specimen ID | Specimen length, L (mm) | Failure modes | Ultimate Load, $P_{EXP}$ (kN) | Average $P_{EXP}$ (kN) |
|---|---|---|---|---|
| C1-ITF-N50-1 | 260 | Web crushing | 16.73 | 15.57 ± 1.16 |
| C1-ITF-N50-2 | 260 | Web crushing | 14.41 | |
| C2-ITF-N50-1 | 195 | Web buckling | 6.68 | 6.24 ± 0.24 |
| C2-ITF-N50-2 | 195 | Web buckling | 6.20 | |
| C3-ITF-N50-1 | 290 | Web buckling | 6.18 | 7.43 ± 1.25 |
| C3-ITF-N50-2 | 290 | Web buckling | 8.67 | |

**Table 3: Failure modes and ultimate web crippling loads in ITF specimens.**

### 2.4 Test setup and method

In accordance of the NAS's [19] recommendation, web crippling experiments were conducted under ETF and ITF loadings. Bearing plates of 200 mm width were positioned in such a way that the loading centreline passes through the web centreline. Using a UTM of 250 kN (make: Bangalore Integrated System Solutions, India), tests were performed. Rate of loading for all tests was fixed at 1mm/min.

## III. EXPERIMENTAL RESULTS

### 3.1 General

In the current experimental study, 6 specimens were tested under ETF loading and same numbers of specimens were tested under ITF loading. Their load-displacement behaviour, ultimate loads and failure patterns have been assessed and detailed discussion is presented in the subsequent sub-sections.

### 3.1 Failure patterns

The failure modes observed in the channel sections were mainly web crushing and web buckling failures influenced by the web slenderness ratio of the sections. In case of C1-section (web slenderness ratio, $\lambda_w$ = 11.8) web crushing was seen in the web of the specimens for both ETF and ITF loading configurations. For instance, multiple longitudinal/horizontal cracks can be seen in the web of specimens in series "C1–ETF–N50" (see Fig. 1a), which are indicative of web crushing failure.

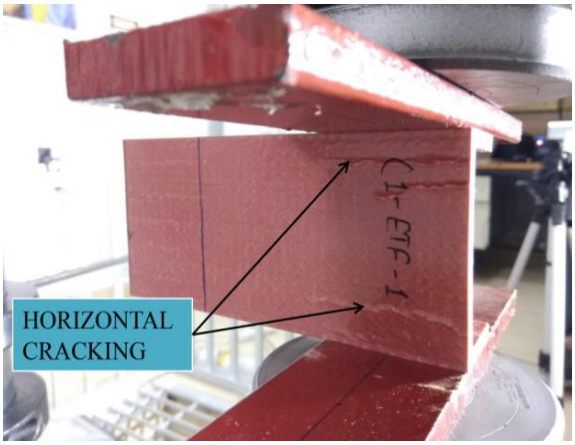
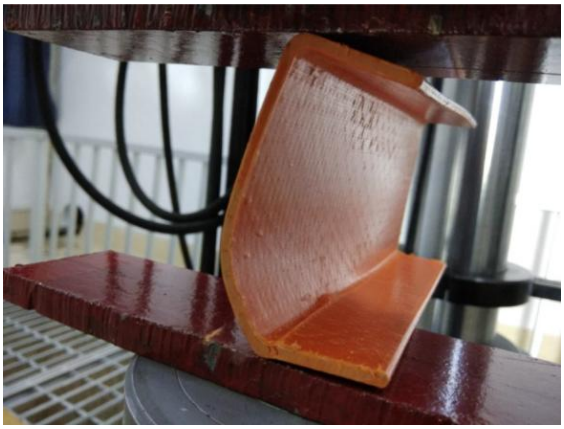



**Figure 1(a): Web crushing failure mode of specimen in 'C1–ETF–N50' series.**

On the other hand, the failure modes in specimens obtained from 'C2' ($\lambda_w$ = 14.0) and 'C3' ($\lambda_w$ = 24.3)-section profiles were dominated by web buckling under both loadings. As can be seen from Figs. 1b–c, specimens in series "C2–ETF–N50" and "C3–ETF–N50" exhibited initial out of plane deformation or web buckling in their webs. After increasing the load for some time, web-flange junction failure occurred that could be seen in the loading region. In the same way, in case of specimens tested under ITF loading, web buckling failure could be observed. The failure patterns observed in the specimens are provided in Tables 2 and 3.



(b)



(c)

**Figure 1(b–c): Failure modes in (b) 'C2–ETF–N50' and (c) 'C3–ETF–N50' series.**

### 3.2 Load–displacement behaviour

Representative load–displacement behaviour under both loading configurations have been shown in Figs. 2a–c for C1, C2 and C3 specimens, respectively. Linear behaviour can be seen in case of "C1–ETF–N50" and "C1–ITF–N50" specimens (see Fig. 2a), where, the load linearly increased upto a certain point followed by a sudden drop in the load. The initial and final peak points in the curves are suggestive of initial failure commencing with single crack followed by ultimate failure by exhibiting multiple cracks in the webs. In case of "C2–ETF–N50" and "C2–ITF–N50" specimens (see fig. 2b), the load–displacement curves showed initial linear behaviour upto initial peak followed by nonlinear behaviour. The nonlinear behaviour in the curves can be linked to the initial web buckling failure. The drop in the load after the final peak is indicative of occurrence of web-flange junction failure. Observations of similar nature can also be found in "C3–ETF–N50" and "C3–ITF–N50" specimens (see fig. 2c).

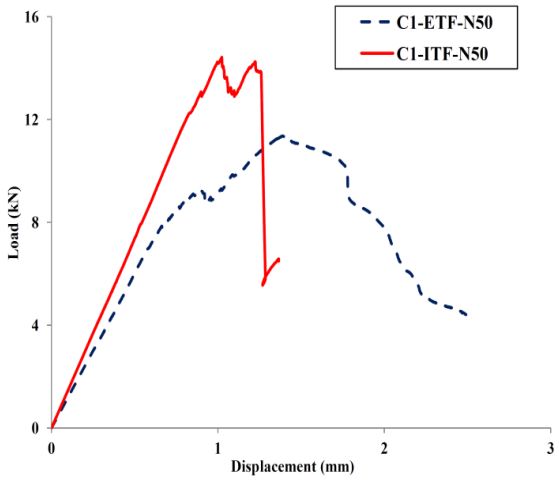
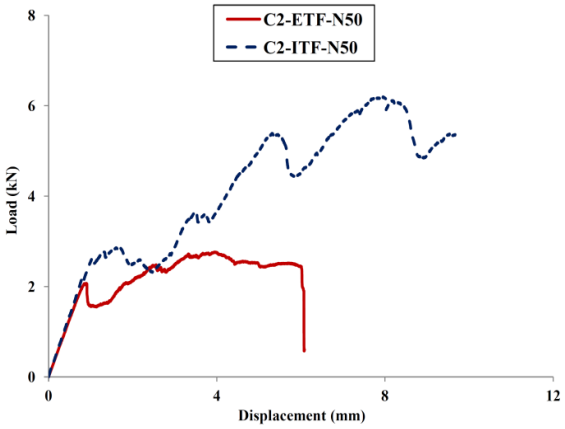


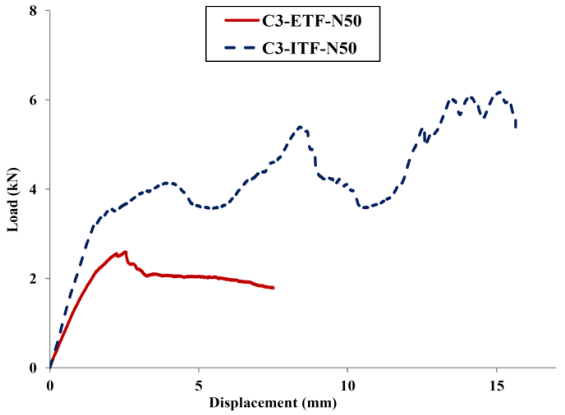

**Figure 2(a): Representative load-displacement plots of C1 specimens for varying loading condition.**

### 3.2 Effect of loading condition

From Figs. 2a–c and Tables 2 and 3, effect of changing loading configuration on the load–displacement behaviour of the GFRP profiles can be understood. From these figures, it can be seen that changing the loading configuration from ETF to ITF increased the load carrying capacity of the specimens. For example, when the loading configuration was changed from ETF to ITF, ultimate load capacity was enhanced by +46.2%, +120.5% and +184.7% for C1, C2 and C3 sections, respectively.




(b)




(c)

**Figure 2(b–c): Load-displacement plots of C2 and C3 specimens for varying loading condition.**

## VIII. CONCLUSION

In the present study, investigation on the performance of GFRP channel profiles under ETF and ITF loading has been reported. A total of 12 specimens were tested and primarily, effect of loading condition and web slenderness ratio on the behaviour of channel beams has been assessed. Mainly, web crushing failure and web buckling failure could be seen in the channel sections that were influenced by the web slenderness ratio. In case of C1 specimens, linear load-displacement behaviour can be seen along with web crushing failure. However, C2 and C3 specimens exhibited nonlinear load-displacement behaviour after initial peak indicating web buckling failure followed by web-flange junction separation. It was also seen that changing the loading condition from ETF to ITF enhanced the ultimate load capacity of the specimens. Changing the loading configuration from ETF to ITF, ultimate load capacity was found to be enhanced by +46.2% (C1), +120.5% (C2) and +184.7% (C3), respectively.

The future work of the present investigation will be aimed at performing numerical investigation and developing design equations for web crippling capacity of GFRP channel beams.

## ACKNOWLEDGEMENTS

Mechanical Engineering Department, Central Instruments Facility and Civil Engineering Department, IIT Guwahati are gratefully acknowledged for extending their support during the tests.

## REFERENCES

[1] Bank LC. Composites for construction: structural design with FRP materials. John Wiley & Sons; 2006 Jul 21.

[2] Nunes F, Correia JR, Silvestre N. Structural behaviour of hybrid FRP pultruded beams: Experimental, numerical and analytical studies. Thin-Walled Structures. 2016 Sep 1;106:201-17.

[3] Fernandes LA, Gonilha J, Correia JR, Silvestre N, Nunes F. Web-crippling of GFRP pultruded profiles. Part 1: Experimental study. Composite Structures. 2015 Feb 1;120:565-77.

[4] Wu C, Zhang LT, Bai Y, Zhao XL. Web crippling behaviour of pultruded GFRP channel sections under transverse bearing load. Composite Structures. 2019 Feb 1;209:129-42.

[5] Haloi, J., Mushahary, S.K., Borsaikia, A.C. and Singh, K.D., 2021. Experimental investigation on the web crippling behaviour of pultruded GFRP wide-flange sections subjected to two-flange loading conditions. Composite Structures, 259, p.113469.

[6] Haloi, J., Borsaikia, A. C. and Singh, K. D., 2022. Effect of web perforation on the performance of pultruded GFRP wide-flange section profile in web crippling under end-two-flange loading configuration. Thin-Walled Structures, 175, p.109187.

[7] Haloi, J., Borsaikia, A.C. and Singh, K.D., 2021. Web crippling behaviour of web perforated GFRP wide-flange sections subjected to interior-two-flange loading condition. Thin-Walled Structures, 166, p.108072.

[8] Fernandes LA, Nunes F, Silvestre N, Correia JR, Gonilha J. Web-crippling of GFRP pultruded profiles. Part 2: Numerical analysis and design. Composite Structures. 2015 Feb 1;120:578-90.

[9] Chen Y, Wang C. Test on pultruded GFRP I–section under web crippling. Composites Part B: Engineering. 2015 Aug 1;77:27-37.

[10] Zhang W, Chen Y. Tests on GFRP pultruded profiles with channel section subjected to web crippling. Applied Composite Materials. 2017 Aug 1;24(4):849-62.

[11] Almeida-Fernandes, L., Correia, J.R. and Silvestre, N., 2021. Effect of fibre layup and bearing length on the web-crippling behaviour of pultruded GFRP profiles. Composite Structures, 267, p.113884.

[12] Wu, C., Zhang, L.T., Tam, L.H., Yan, L. and He, L., 2020. Effect of bearing length on web crippling behavior of pultruded GFRP channel section. Composite Structures, 253, p.112810.

[13] ASTM D2584-18. Standard test method for ignition loss of cured reinforced resins. In American Society for Testing and Materials.
[14] Haloi, J., Borsaikia, A.C. and Singh, K.D., 2022. Mechanical characterization of pultruded GFRP channel, wide flange and rectangular hollow profiles. Innovative Infrastructure Solutions, 7(1), pp.1-18.
[15] ASTM D3039-17. Standard test method for tensile properties of polymer matrix composite materials. ASTM International; 2017.
[16] ASTM D2344-16. Standard test method for short-beam strength of polymer matrix composite materials and their laminates. ASTM International; 2016.
[17] Hodgkinson JM, editor. Mechanical testing of advanced fibre composites. Elsevier; 2000 Oct 27.
[18] ASTM D 3410. Standard test method for compressive properties of polymer matrix composite materials with unsupported gage section by shear loading. West Conshohocken, Pennsylvania, USA: ASTM International; 2006.
[19] North Amercian Specifications for the Design of Cold-Formed Steel Structural Members. AISI S100-16, American Iron and Steel Institute, Washington, DC. 2016.

★★★